Biochemical and Biophysical Research Communications 446 (2014) 541–548

Contents lists available at ScienceDirect

Biochemical and Biophysical Research Communications

journal homepage: www.elsevier.com/locate/ybbrc

Anti-miR-197 inhibits migration in HCC cells by targeting KAI 1/CD82

Weiqi Dai [a,1], Chengfen Wang [a,1], Fan Wang [a,1], Yugang Wang [b], Miao Shen [a], Kan Chen [a], Ping Cheng [a], Yan Zhang [a], Jing Yang [a], Rong Zhu [a], Huawei Zhang [a], Jingjing Li [a], Yuanyuan Zheng [a], Jie Lu [a], Yingqun Zhou [a], Ling Xu [b,*], Chuanyong Guo [a,*]

[a] Department of Gastroenterology, Shanghai Tenth People's Hospital, Tongji University, School of Medicine, Shanghai, China
[b] Department of Gastroenterology, Tong Ren Hospital, Jiaotong University, School of Medicine, Shanghai, China

ARTICLE INFO

Article history:
Received 24 February 2014
Available online 12 March 2014

Keywords:
miR-197
CD82
Hepatocellular carcinoma
Metastasis

ABSTRACT

Aim: To investigate the metastatic effects and mechanisms of miR-197 in hepatocellular carcinoma (HCC).

Methods and results: The levels of miR-197 increased in HCC cells and tissues compared with a normal hepatic cell line (LO2) and adjacent nontumorous liver tissues, respectively. miR-197 expression negatively correlated with CD82 mRNA expression in these cell lines and tissues. Dual luciferase reporter assay and Western blot confirmed a direct interaction between miR-197 and CD82 3′UTR sequences. After miR-197 was silenced in HCC cells, CD82 expression increased. In the presence of human hepatocyte growth factor (HGF), cells silenced for anti-miR-197 exhibited elongated cellular tails and diminished lamellipodia due to reductions in both ROCK activity and the levels of Rac 1 protein. Downregulation of miR-197 along with the upregulation of CD82 in HCC cells resulted in the inhibition of HCC migration and invasion *in vitro* and *in vivo*.

Conclusion: Taken together, these data suggest that anti-miR-197 suppresses HCC migration and invasion by targeting CD82. The regulation of the miR-197/CD82 axis could be a novel therapeutic target in future HCC effective therapy.

1. Introduction

Hepatocellular carcinoma (HCC) is a major health problem around the world. Because of high tumor recurrence and mortality, current HCC standard practices such as liver transplantation and surgical resection are less than satisfactory [1–4]. Thus, it is essential to search for molecular markers, such as miRNA, that can predict recurrence of HCC.

The mechanisms involved in the development of HCC are multifactorial, including the interactions between various tumor suppressor genes, oncogenes, cell adhesion molecules and growth factors [5]. Increased evidence suggests that KAI 1/CD82 is a metastasis suppressor factor during HCC carcinogenesis [6]. KAI 1/CD82 is expressed in various human tissues, and it is worth noting that a reduction of both its mRNA and protein expression is found in many advanced stages of tumors. For example, in lung tumor patients, several studies have determined that CD82 mRNA expression is related to a better prognosis, while its suppression is related to distant metastases in many pancreatic cancer patients [7]. Thus, in many tumors, including HCC, identifying a reagent that can modify the levels of CD82 would provide an additional method to treat liver cancer.

MicroRNAs (miRNAs) are a series of small non-coding RNAs well conserved in animals and plants [9] that have vital roles in processes such as cellular differentiation, cell-cycle control, proliferation, and cell death [8]. Given that 50% of miRNAs are located in cancer-related genomic regions, including fragile sites [10], they may play a vital role in cancer pathogenesis. The miRNAs involved in tumorigenesis are considered to be oncogenic miRNAs. In particular, miR-197 has been investigated in various types of cancer. Compared to the adjacent normal tissue, squamous cell carcinoma of the tongue was shown to overexpress miR-197 [11]. In addition, based on its pattern of expression, it is possible to differentiate malignant diseases from benign indeterminate thyroid lesions on fine needle aspiration (FNA) [12]. However, the roles of miR-197 and its targets in HCC have not yet been reported.

* Corresponding authors. Address: Department of Gastroenterology, Shanghai Tenth People's Hospital, Tongji University, School of Medicine, 301 Yanchang Road, Shanghai 200072, China (C. Guo).
E-mail addresses: xuling606@sina.com (L. Xu), guochuanyong@hotmail.com (C. Guo).
[1] Weiqi Dai, Chengfen Wang, and Fan Wang contributed equally to this article.

http://dx.doi.org/10.1016/j.bbrc.2014.03.006
0006-291X/

In our study, we determined that CD82 is a target of miR-197 and that downregulation of miR-197 inhibits HCC cell migration and invasion *in vitro* and *in vivo*. Therefore, our results suggest a potential medical value of the miR-197/CD82 axis in HCC effective therapy.

2. Materials and methods

2.1. Reagents

Human hepatocyte growth factor (HGF) was purchased from Sigma–Aldrich. The primary antibodies against β-tubulin, Rac 1, and CD82 were purchased from Abcam.

2.2. Cell culture and morphological analysis

The experimental cell lines were purchased from the Chinese Academy of Sciences Committee Type Culture Collection cell bank. The cell lines were maintained in high glucose DMEM (Thermo Fisher) supplemented with 10% FBS at 37 °C in 5% CO_2.

Cellular morphology was observed by a phase contrast microscope and was imaged by digital photography.

2.3. Tissue samples

Fresh HCC tissues and their adjacent normal samples were gained from 7 patients who underwent liver resection surgery between January 2012 and September 2013 at Shanghai Tenth People's Hospital. HCC diagnosis was based on World Health Organization criteria [13]. Ethical approval was obtained from the research ethics committee of Shanghai Tenth People's Hospital and written informed consent was gained from every patient.

2.4. Plasmid construction and luciferase reporter assay

Potential target binding sequences of hsa-miR-197 in the 3′UTR of CD82 mRNA was searched using TargetScan. The full length 3′UTR of CD82 (Genbank Accession: NM_002231.3) was produced by annealing the sense strand to form 5′ Xhol and 3′ Not I sites which were used for ligation into psiCHECK-2 dual-luciferase reporter plasmid with the stop codon including the Renilla luciferase gene. The exact sequences binding to has-miR-197 from 3′UTR of CD82 was mutated at the position of 443–445 and 452–457 from TGG to CAT and from TGGTGA to CAAGTC, respectively.

For luciferase reporter assay, after 48 h transfection, a dual luciferase reporter assay system (Promega) was used to test cellular luciferase activity according to the manufacturer's protocol. The luciferase activity was examined by a Lumat 9507 illuminometer (Berthold). Relative luciferase activity was normalized by Renilla luciferase activity of psi-CHECK-2 plasmid.

2.5. Construction of stable HCC cell lines expressing short hairpin lentiviral vector

The short hairpin RNAs targeting miR-197 were inserted into the pGreenPuro™ shRNA expression lentivector (SBI). The short hairpin RNAs were designed to be asymmetric and were expressed by the H1 promoter. The cop green fluorescence protein in this vector was also used for the selection of stably transfected cells. Pseu doviral particles were obtained in the 293TN cell line by the pPACK-H1 Lentivector Packaging System (SBI) according to the manufacturer's protocol.

2.6. RNA interference (RNAi) of CD82

HCC cells were transfected with 50 nM CD82 siRNA or control siRNA with Lipofectamine 2000 (Invitrogen). After 48 h of transfection, the cells were processed for the quantification of specific RNAs and proteins. CD82 siRNA: 5′-UAUUUGGUGACUUUGAUACAGGCUG-3′.

2.7. Cell counting kit-8 (CCK-8) assays

HCC cells were treated with the indicated treatments in 96-well plates. 10 μl of the CCK-8 solution (Peptide Institute Inc., Osaka, Japan) was added to each well of the plate. After the plate was cultured for 4 h in the incubator, the absorbance was measured at 450 nm using a microplate reader.

2.8. RNA extraction and qRT-PCR

First-strand cDNA was synthesized from 2 μg of total RNA. Amplification and detection were tested using the ABIPRISM 7900 Sequence Detection System (Applied Biosystems) starting with 1 μl cDNA and SYBR Green Real-time PCR Master Mix (Takara). The comparative cycle threshold (Ct) method was employed to analyze the relative expressions of CD82 and miR-197.

2.9. Immunobloting

Cellular and tissular total proteins were extracted by radioimmunoprecipitation assay (RIPA) buffer. For reducing gel electrophoresis, equal amounts of samples were added to each lane. The samples were then resolved by SDS–PAGE and transferred to polyvinyl difluoride membranes. The membranes were sequentially blocked with 5% defatted milk, and incubated with specific primary antibodies and fluorescent anti-mouse/rabbit secondary antibodies. Li-COR ODYSSEY scanner (LICOR) was used to detect the antigens on the blots.

2.10. Transwell migration and invasion assays

For the migration assay, HCC-LM3 and MHCC-97H cells (5×10^4) were seeded in high glucose DMEM supplemented with 0.2% FBS to the upper chamber of a 8.0-μm pore membrane Boyden chamber (Costar, Cambridge, MA). The lower chamber contained high glucose DMEM medium with 10% FBS in a 24-well culture plate. After cells were cultured for 24 h, migrating cells were stained with crystal violet.

For the invasion assay, a Matrigel (BD, MA)-coated 8.0-μm pore membrane Boyden chamber was used. The inserts were pre-coated with 100 μl of 1 mg/ml Matrigel matrix at 37 °C for 4 h. The procedures used in the cell invasion assay were similar to those of the migration assay.

2.11. Rac1 GPTase and Rho kinase (ROCK) activity assays

Intracellular Rac1 activity was examined by StressXpress Rac1 Activation Kit (StressGen, Victoria, Canada) according to the manufacturer's instructions. As preparation for the experiment, HCC cells were left untreated in serum free medium for 24 h at 37 °C in 5% CO_2. After incubation, HCC cells were lysed on ice for 5 min. Equal amounts of cellular lysate were incubated with the GST-Pak-PBD in the spin cup at 4 °C for 60 min. Non-binding proteins were wiped by centrifuging the spin cup at 7200*g* for 1 min. The total cell lysates and the affinity-precipitated proteins were then immunoblotted for Rac1.

The ROCK activities in cells were tested by using MBL Rho Kinase Assay Kit (MBL International, Woburn, MA) according to the manuscript protocols.

2.12. Animal experiments

Four-week-old male athymic BALB/c nu/nu mice were obtained from Shanghai SLAC Laboratory Animal Co. Ltd. (Shanghai, China).

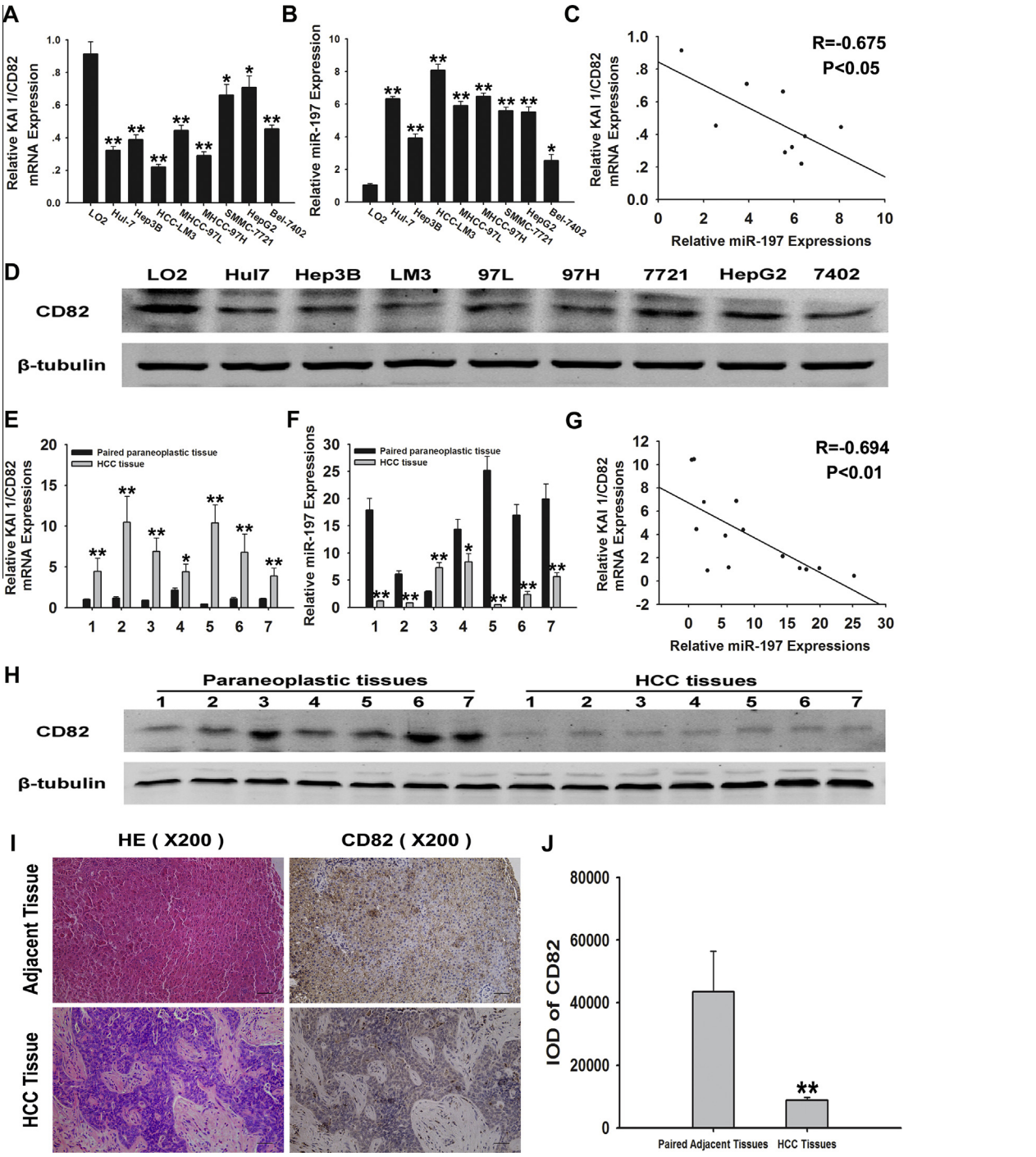

Fig. 1. mRNA and protein expression of CD82 in HCC cells and tissues. (A, B, E, and F) Relative miR-197 and CD82 mRNA expressions in HCC cells and tissues by qRT-PCR. Values represent means ± SEMs ($^{*}P < 0.05$ and $^{**}P < 0.01$; $n = 3$). (C, G) Statistical correlations between the expressions of miR-197 and CD82 mRNA in HCC cells and tissues were analyzed by Spearman's test in SPSS 17.0 software ($R = -0.675, -0.694$; $P < 0.05, 0.01$; respectively). (D, H) CD82 protein expression in HCC cells and tissues. β-Tubulin was used as an internal control. A representative image of three independent experiments is shown. (I) Hematoxylin–eosin staining of primary HCC and the adjacent tissues was used in the diagnosis of HCC. Representative immunoreactivity to CD82 was observed in the plasma membrane of tumorous and adjacent non-tumorous (200×). Bars, 50 μM. (J) The integrated optical density (IOD) of CD82 were analyzed by Image-Pro Plus 6.0. Data are showed as means ± SEMs ($^{**}P < 0.01$; $n = 3$).

All trials were approved by the Animal Care and Use Committee of The Tenth People's Hospital of Shanghai and were conducted according to the National Institutes of Health "Guide for the Care and Use of Laboratory Animals". Lenti-anti-miR-197 or EV-infected HCC-LM3 cells (5×10^6) suspended in 0.2 ml of serum free culture medium were subcutaneously injected into the upper flank region of nude mice. After 2 weeks, the subcutaneous tumor, which was 1.0 cm in diameter, was cut into pieces of about 1.0 mm^3, which were then inserted into the livers of another 10 nude mice. Of the 10 nude mice, 5 were randomly selected for the Lenti-anti-miR-197 group and the remaining 5 were chosen for the EV vehicle group. The mice were followed for 30 days and then killed by cervical dislocation. Livers and lungs were resected and pictured by high-definition digital camera.

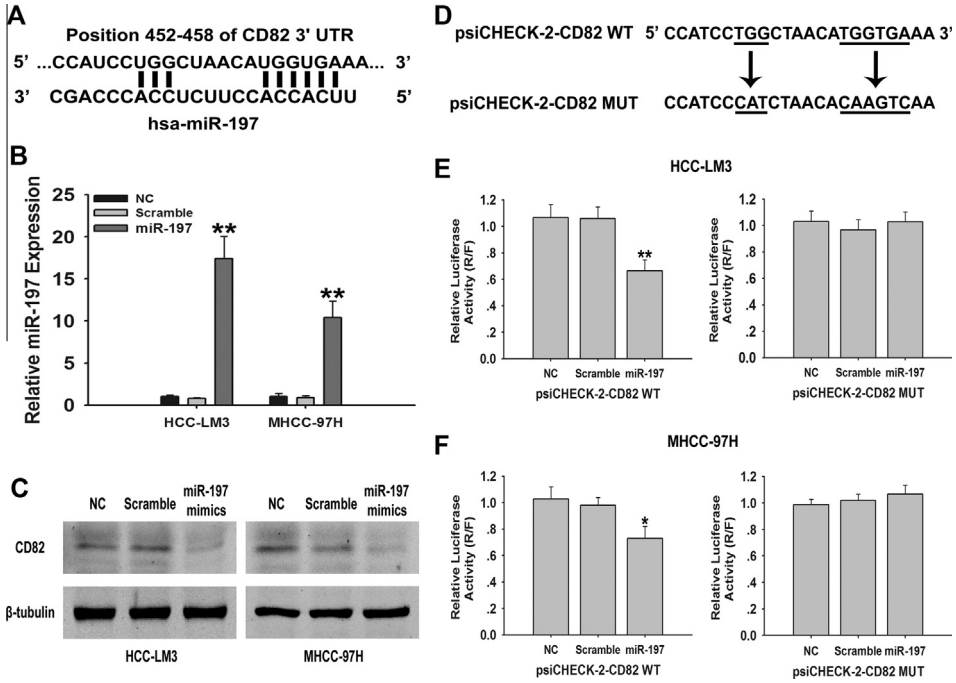

Fig. 2. miR-197 directly regulates the expression of CD82. (A) The highly conserved mature miR-197 sequence in mammals and the alignment sequences between miR-197 and CD82 3′UTR are shown. (B, C) miR-197 and protein expression of CD82 were examined by qRT-PCR and Western blotting in HCC cells. The experiment was repeated three times and representative samples are shown. Values represent means ± SEMs ($^{**}P < 0.01$; $n = 3$). (D) Sequence of the psiCHECK-2 CD82 wild type and the mutant that disrupts the interaction with miR-197 are shown. (E, F) The histogram bars represent the relative dual luciferase activity after HCC cells were transfected with miR-197 mimics or control miRNAs. Values represent means ± SEMs ($^{*}P < 0.05$ and $^{**}P < 0.01$; $n = 5$).

2.13. Immunohistochemistry

Paraffin blocks were cut into 5 μm thick sections, mounted onto slides. The sections were deparaffinized by xylene, rehydrated by graded alcohol, and heated at 95 °C for 20 min in Tris–EDTA buffer (pH 9.0) for antigen exposure. The tissue sections were then incubated in 0.3% Dako REAL Peroxidase-Blocking Solution (Dako) and goat normal serum for 30 min, respectively. Primary antibodies were incubated with the samples overnight at 4 °C. After washing with PBS/0.1% Tween 20, the sections were incubated with horseradish peroxidase-conjugated rabbit-specific IgG (Dako) diluted in 1:300 for 1 h at 37 °C. The sections were washed with PBS/0.1% Tween 20 again and 3,3-diaminobenzidine substrate chromogen solution was applied, followed by counterstaining nucleus with Meyer's haematoxylin.

2.14. Statistical analysis

Statistical analysis was performed with SPSS 17.0 software and was carried out using a two-tailed unpaired Student's *t*-test. The relationship between miR-197 and CD82 mRNA expression was analyzed using the Spearman's test. Values are expressed as the means ± standard deviation. Values of $^{*,\#}P < 0.05$ and $^{**,\#\#}P < 0.01$ were considered statistically significant.

3. Results

3.1. miR-197 and CD82 expression in HCC cells and samples

The expression of the CD82 mRNA and protein was markedly more reduced in 8 HCC cell lines than in the normal hepatic cell lines (Fig. 1A and D). After detection of 7 primary HCC samples by hematoxylin–eosin staining (Fig. 1I), expression of CD82 protein was also observed in the cell membranes of tumor cells (Fig. 1I) by immunohistochemistry. The expression of CD82 mRNA and protein were significantly decreased in the tumors when compared to the adjacent nontumorous liver tissues gained from the same patient (Fig. 1E, H, and J). In contrast, the miR-197 expression was higher in the tumor cells and tissues than in the nontumorous cells and tissues (Fig. 1B and F). The miR-197 level is negatively correlated with the CD82 protein and mRNA expression ($R = -0.675$, -0.694; $P < 0.05$, 0.01; Fig. 1C and G).

3.2. miR-197 directly targets CD82

TargetScan (http://www.targetscan.org/) was used to predict miRNA binding sites within CD82 3′UTR. Based on the previous observations, we hypothesized that the CD82 mRNA might be a direct target of miR-197. By screening the 3′UTR of CD82 mRNA, we identified a possible miR-197 binding site near to position 443–445 and 452–457 (Fig. 2A). Transfection of 50 nM miR-197 mimics in HCC-LM3 and MHCC-97H cells resulted in the enhancement of miR-197 and reduction of CD82 protein expression in both cell lines significantly compared to the control groups (Fig. 2B and C). To determine direct impact of miR-197 on 3′UTR sequence of CD821 mRNA, we employed the dual luciferase reporter assay. The relative luciferase activity of psiCHECK-2-CD82 WT reporter was markedly reduced by miR-197 mimics, while psiCHECK-2-CD82 MUT (Fig. 2D) displayed no effect by comparison with the control group (Fig. 2E and F). Based on these data, we conclude that CD82 is directly regulated by miR-197.

3.3. Generation of stable Lenti-anti-miR-197-HCC-LM3 and -MHCC-97H cell lines

Stable cell lines Lenti-anti-miR-197-HCC-LM3 and -MHCC-97H were obtained. GFP fluorescence staining was used to measure the efficiency of transfection and transduction (Fig. 3A). The transfection and transduction efficiency were also tested by qRT-PCR (Fig. 3B). The miR-197 expression in Lenti-anti-miR-197 groups was significantly decreased. Concomitantly, CD82 protein

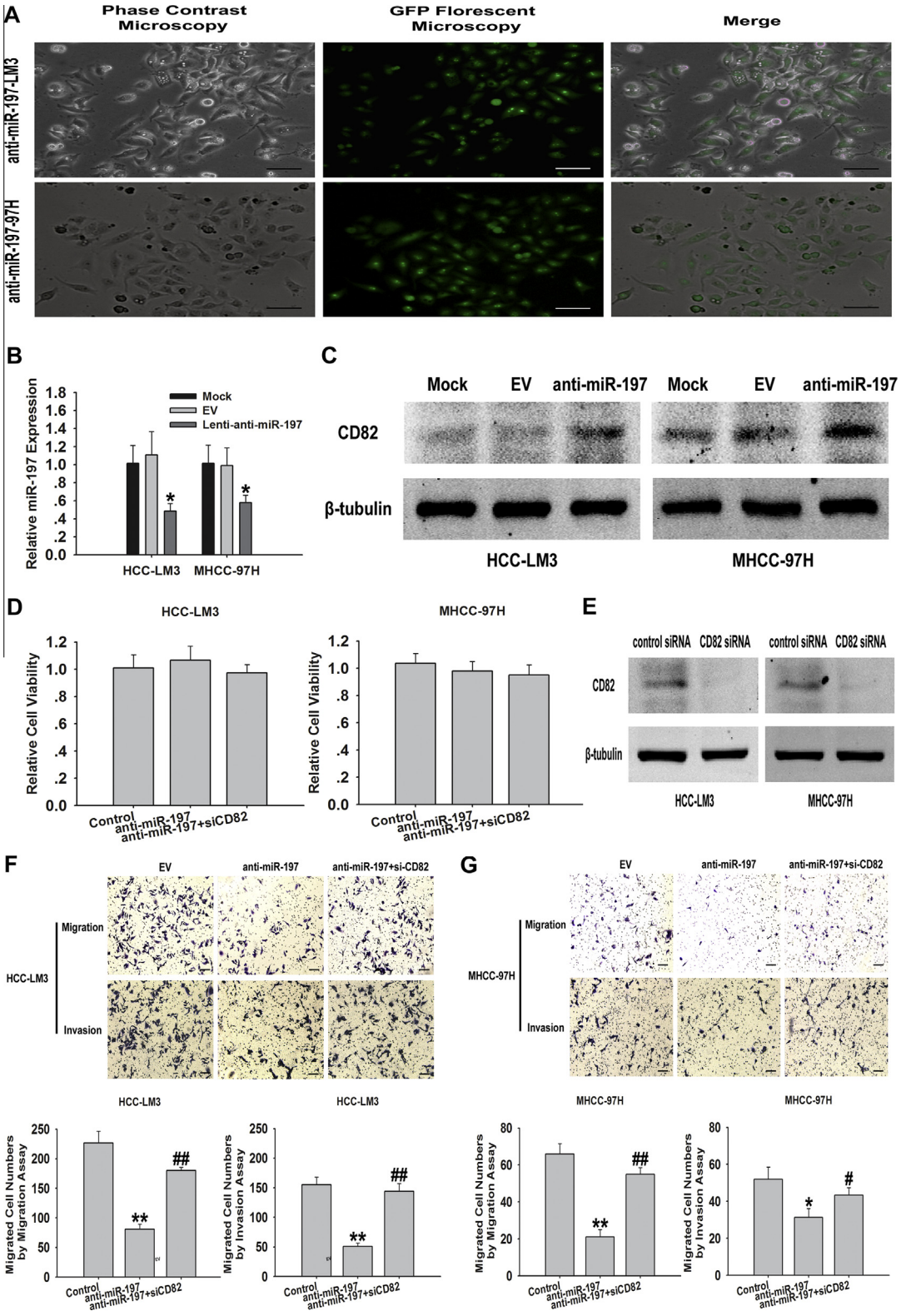

Fig. 3. (A, B) Transduction efficiency was tested by fluorescent microscopy (X200) and qRT-PCR after HCC cells were transduced with pGreenPuro™ shRNA expression lentivector encoding anti-miR-197 for 72 h. Values represent means ± SEM ($^{*}P < 0.05$; $n = 3$). Bars, 50 μM. (C) CD82 protein expression was detected by Western blot. The representative images of three independent experiments are shown. (D) In different groups, CCK-8 assay was used to test cellular viability in HCC cells ($n = 3$). Error bar shows standard error. (E) After HCC-LM3 and MHCC-97H cells were transfected with CD82 siRNA for 48 h, the representative protein expression of CD82 was examined. (F, G) Transwell migration and invasion assays were employed in two HCC samples. The representative images (100×) are shown. Bars, 50 μM. The histograms plot numbers of migrating or invading cells to the lower chamber from three independent experiments. Values represent means ± SEM ($^{*}P < 0.05$ *vs.* EV group; $^{**}P < 0.01$ *vs.* EV group; $^{\#}P < 0.05$ *vs.* anti-miR-197 group; $^{\#\#}P < 0.01$ *vs.* anti-miR-197 group; $n = 3$).

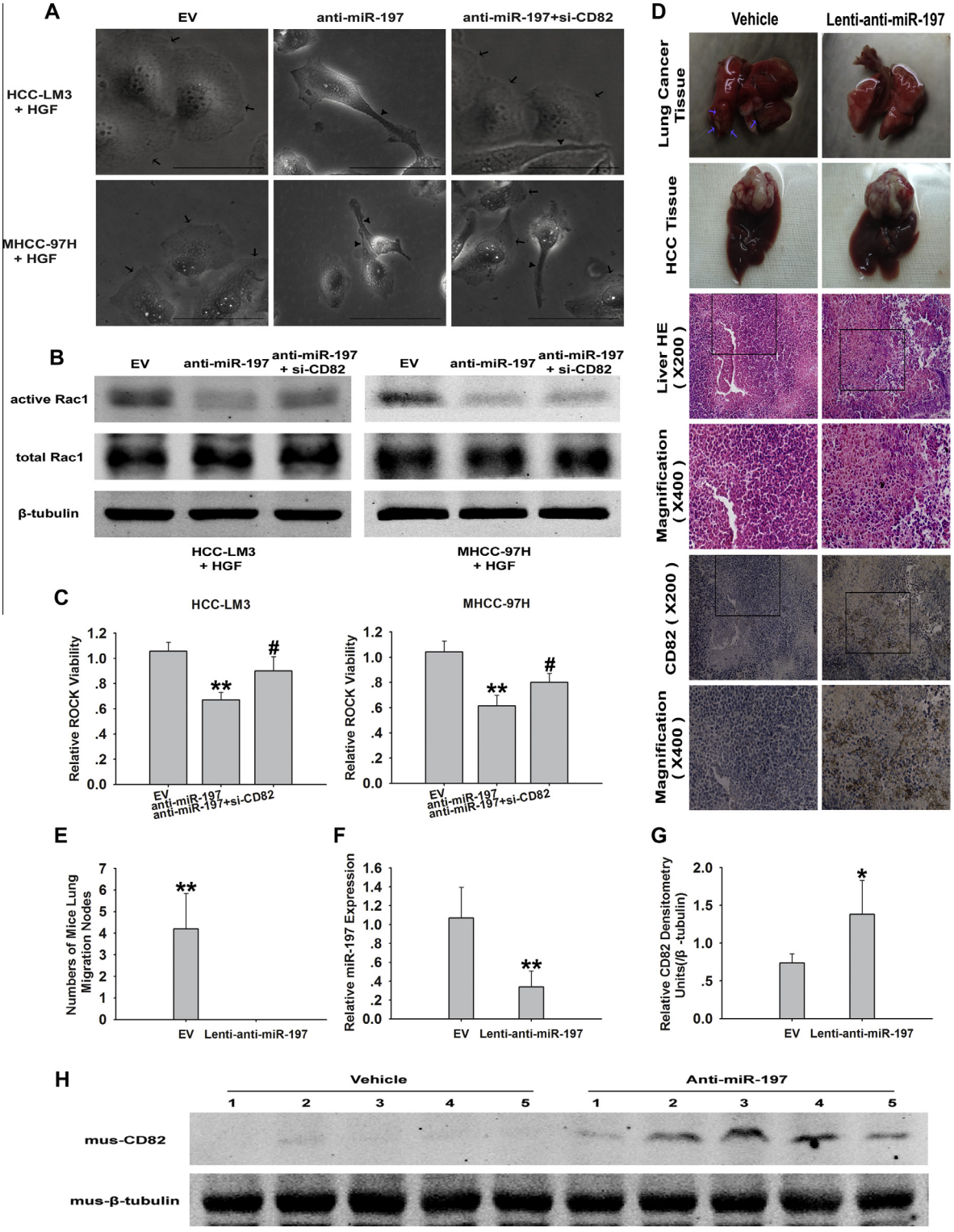

Fig. 4. The migration inhibitory effects and mechanisms of anti-miR-197 in HCC nude mice model and HCC cells. (A) After HCC cells were cultured in HGF (50 ng/ml) for 6 h, HCC-LM3 and MHCC-97H cells from different groups were pictured by microscopy. Representative images were displayed. Bars, 50 μM. The arrow and triangle indicated lamellipodia and elongated cellular extensions, respectively. (B) Protein expressions of total/activated Rac1 in HCC cells were tested by Western blot. Representative images are shown. (C) The results shown in the histogram are the relative ROCK activity measured with the MBL Rho Kinase Assay kit in three individual experiments ($^{**}P < 0.01$ *vs.* EV group; $^{\#}P < 0.05$ *vs.* anti-miR-197 group; $n = 3$). (D) At the end of the experiments with animals, representative mice lung and liver images of EV and lenti-anti-miR-197 group were taken. Liver hematoxylin and eosin staining and CD82 immunostaining images are also included. Bars, 50 μM. (E) The histogram represents the numbers of pulmonary metastases in both groups. (F) miR-197 expressions in EV and lenti-anti-miR-197 group by qRT-PCR. Values represent mean ± SEM ($^{**}P < 0.01$; $n = 3$). (G, H) The tumorous protein amounts of CD82 from EV and lenti-anti-miR-197 groups were assayed by Western blot. The representative images were shown. β-Tubulin was used as a loading control. The upper part showed the related densitometry analysis ($^{*}P < 0.05$; $n = 3$). Error bar shows standard error.

level was markedly increased compared to the mock and EV groups in HCC-LM3 and MHCC-97H cell lines (Fig. 3C).

3.4. Anti-miR-197 inhibits migration and invasion activities through CD82 expression in HCC cells

CD82 siRNA significantly reduced the protein expression of CD82 compared to the mock and control siRNA groups (Fig. 3E). Furthermore, Lenti-anti-miR-197 significantly reduced cellular migration and invasion activities compared to the EV group, an effect that was reversed by the addition of CD82 siRNA to the Lenti-anti-miR-197-expressing HCC-LM3 and MHCC-97H cell lines (Fig. 3F and G). To avoid the influence of cellular inhibitory functions, we further examined the cellular inhibitory effects by the CCK-8 assay in these groups. Data showed that there were no marked cytotoxicity between them (Fig. 3D).

3.5. Anti-miR-197 induces cell aberrant morphology through ROCK activity and activated Rac1 protein suppression

HCC cells were cultured in DMEM containing 10% FBS and HGF (50 ng/ml) at 37 °C for 6 h. We noticed two morphological changes in anti-miR-197 groups by comparison with the EV group in HCC cells. First, the lamellipodia formation in anti-miR-197 groups was completely lost or typically limited to the one or two cellular ends, in contrast to the widespread and fan-like lamellipodia in the EV cells (Fig. 4A). The destroyed lamellipodia could result from fewer protrusive activities during cell migration and invasion [14]. The lack of lamellipodia formation in the anti-miR-197 groups was partly reversed by the expression of a CD82 siRNA. Data were consistent with articles showing that the expression of CD82 reduced lamellipodia formation [15–17]. Second, in anti-miR-197 groups extraordinarily elongated cellular extensions could be observed (Fig. 4A). The frequency of these extensions in antimiR-197 groups (29%) was much higher than that in EV groups (9%, Student's t-test, $n = 3$, $P < 0.01$). According to Liu et al. [14], the elongated cellular extensions are caused by a lack of contractile retraction. The frequency of extraordinarily elongated cellular extensions was inhibited in anti-miR-197 groups when CD82 siRNA was also added (Fig. 4A). Compared to control groups, the total Rac1 protein level in anti-miR-197 groups was not changed in HCC-LM3 and HepG2 cells after these were incubated in HGF for 6 h. However, the protein expression of activated Rac1 and ROCK activity were significantly decreased in anti-miR-197 groups compared to the EV groups, while they were upregulated in the presence of both anti-miR-197 and CD82 siRNA (Fig. 4B and C).

3.6. HCC metastasis inhibitory effects and mechanisms of anti-miR-197 in vivo

At the end of the *in vivo* experiment, miR-197 expression was significantly reduced in the lenti-anti-miR-197 group compared to the EV group (Fig 4F). The numbers of lung metastatic nodes in the lenti-anti-miR-197 group were lower than that in the EV vehicle group (Fig 4D). Western blots and immunohistochemistry staining indicated that, by comparison with the EV vehicle group, the lenti-anti-miR-197 group significantly increased the protein levels of CD82 in the liver tissues of nude mice (Fig 4D, G, and H).

4. Discussion

HCC is among the top ten prevalent cancers around the world [1]. Hepatic metastasis is the major cause leading to its poor prognosis [7]. Therefore, it is essential to understand the molecular mechanisms underlying HCC metastasis and there is great urgency in developing novel therapeutic targets. The deregulation or dysfunction of miRNAs has been shown to be involved in cancer progression, namely in patients with HCC. For example, several miRNAs, including miR-224, miR-106b, miR-21 [18–20], are upregulated in HCC and involved in the development of HCC. Previous research suggested a possible relationship between malignant neoplasms and miR-197 overexpression [11–12,21]. Moreover, in lung cancer, miR-197 also interacted with the 3′UTR of tumor suppressor gene p120 catenin and promoted tumor migration activity [22]. In our study, we found that miR-197 expression was upregulated in both HCC tissues and cell lines in comparison with the adjacent tissues or normal hepatic cells, respectively. Anti-miR-197 significantly inhibited migration and invasion without cytotoxic effects in HCC cell lines. Anti-miR-197 repressed lung cancer metastatic nodes in nude mice liver orthotopic tumor planting metastasis model. We also determined a significant negative correlation between the levels of miR-197 and CD82 mRNA in HCC cells and tissues. Furthermore, using software algorithms and a luciferase reporter assay, we were able to show that the tumor metastasis suppressor CD82 is directly regulated by miR-197.

CD82 was identified as a putative metastasis suppressor in a series of human cancers, including HCC [6]. We also found that the expression of both CD82 mRNA and protein was decreased in HCC cells and tissues. Recent studies reported that CD82 attenuated the pathways derived from c-Met [23–25], integrin [26], epidermal growth factor receptor (EGFR) [27], and FAK-Src-p130CAS-Crk [24,27]. Moreover, Liu et al. demonstrated that CD82 suppressed cell movement by inhibiting the formation of cellular protrusion and retraction [14]. Consistent with the previous study, we demonstrated that in the presence of HGF anti-miR-197 reduced formation of lamellipodia and generated cellular elongated trailing tail through enhanced CD82 protein expression. Furthermore, both Rac1 and ROCK activities, which are responsible for the formation of lamellipodia and elongated cellular extensions, respectively [14], were markedly decreased by anti-miR-197.

It was previously reported that miR-197 negatively regulates tumor suppressor gene FUS 1 in lung cancer [21]. miR-197 also promoted the metastasis activity of pancreatic cancer cells by targeting p120 Catenin [22]. These results suggested that single miRNA can target several mRNAs to mediate gene expression at the post-transcriptional level. In this context, it is important to stress that the luciferase assay in HCC cells demonstrated a direct interaction between the CD82 RNA and miR-197.

Finally, our experiments on the roles of miR-197 and CD82 in animal models, highlight the relevance of these line of research for the clinical treatment of patients with HCC.

In conclusion, our study proved that downregulation of the miR-197 expression and the subsequent overexpression of CD82 inhibited metastasis of HCC. These data indicate that miR-197 and its downstream target could be useful as tumor prognostic markers and/or therapeutic targets in HCC.

Conflict of interests

The authors declare no conflict of interest.

Acknowledgment

This Project was supported by the National Natural Science Foundation of China (Grant No. 81270515).

References

[1] F. Wang et al., Salinomycin inhibits proliferation and induces apoptosis of human hepatocellular carcinoma cells in vitro and in vivo, PLoS One 7 (2012) e50638.

[2] L. Jie et al., The hippo-yes association protein pathway in liver cancer, Gastroenterol. Res. Pract. 2013 (2013) 187070.
[3] W. Dai et al., Genistein inhibits hepatocellular carcinoma cell migration by reversing the epithelial–mesenchymal transition: partial mediation by the transcription factor NFAT1, Mol. Carcinog. (2013), http://dx.doi.org/10.1002/mc.22100 (Epub ahead of print).
[4] P. Cheng et al., Ethyl pyruvate inhibits proliferation and induces apoptosis of hepatocellular carcinoma via regulation of the HMGB1-RAGE and AKT pathways, Biochem. Biophys. Res. Commun. 443 (2014) 1162–1168.
[5] K.F. Becker, G. Keller, H. Hoefler, The use of molecular biology in diagnosis and prognosis of gastric cancer, Surg. Oncol. 9 (2000) 5–11.
[6] X.Z. Guo et al., KAI1, a new metastasis suppressor gene, is reduced in metastatic hepatocellular carcinoma, Hepatology 28 (1998) 1481–1488.
[7] H. Tonoli, J.C. Barrett, CD82 metastasis suppressor gene: a potential target for new therapeutics, Trends Mol. Med. 11 (2005) 563–570.
[8] G. Meister, MiRNAs get an early start on translational silencing, Cell 131 (2007) 25–28.
[9] M. Lagos-Quintana, R. Rauhut, W. Lendeckel, T. Tuschl, Identification of novel genes coding for small expressed RNAs, Science 294 (2001) 853–858.
[10] G.A. Calin et al., Human microRNA genes are frequently located at fragile sites and genomic regions involved in cancers, Proc. Natl. Acad. Sci. USA 101 (2004) 2999–3004.
[11] T.S. Wong, X.B. Liu, B.Y. Wong, R.W. Ng, A.P. Yuen, W.I. Wei, Mature miR-184 as potential oncogenic microRNA of squamous cell carcinoma of tongue, Clin. Cancer Res. 14 (2008) 2588–2592.
[12] X.M. Keutgen et al., A panel of four miRNAs accurately differentiates malignant from benign indeterminate thyroid lesions on fine needle aspiration, Clin. Cancer Res. 18 (2012) 2032–2038.
[13] A.W. Ke et al., Role of overexpression of CD151 and/or c-Met in predicting prognosis of hepatocellular carcinoma, Hepatology 49 (2009) 491–503.
[14] W.M. Liu et al., Tetraspanin CD82 inhibits protrusion and retraction in cell movement by attenuating the plasma membrane-dependent actin organization, PLoS One 7 (2012) e51797.
[15] E. Odintsova, T. Sugiura, F. Berditchevski, Attenuation of EGF receptor signaling by a metastasis suppressor, the tetraspanin CD82/KAI-1, Curr. Biol. 10 (2000) 1009–1012.
[16] B. Zhou, L. Liu, M. Reddivari, X.A. Zhang, The palmitoylation of metastasis suppressor KAI1/CD82 is important for its motility- and invasiveness-inhibitory activity, Cancer Res. 64 (2004) 7455–7463.
[17] M. Takahashi, T. Sugiura, M. Abe, K. Ishii, K. Shirasuna, Regulation of c-Met signaling by the tetraspanin KAI-1/CD82 affects cancer cell migration, Int. J. Cancer 121 (2007) 1919–1929.
[18] C. Scisciani et al., Transcriptional regulation of miR-224 upregulated in human HCCs by NFκB inflammatory pathways, J. Hepatol. 56 (2012) 855–861.
[19] G. Shen, H. Jia, Q. Tai, Y. Li, D. Chen, MiR-106b downregulates adenomatous polyposis coli and promotes cell proliferation in human hepatocellular carcinoma, Carcinogenesis 34 (2013) 211–219.
[20] Q.J. Li et al., MicroRNA-10b promotes migration and invasion through CADM1 in human hepatocellular carcinoma cells, Tumour Biol. 33 (2012) 1455–1465.
[21] L. Du et al., MiR-93, miR-98, and miR-197 regulate expression of tumor suppressor gene FUS1, Mol. Cancer Res. 7 (2009) 1234–1243.
[22] S. Hamada et al., MiR-197 induces epithelial–mesenchymal transition in pancreatic cancer cells by targeting p120 catenin, J. Cell. Physiol. 228 (2013) 1255–1263.
[23] A.R. Todeschini, J.N. Dos Santos, K. Handa, S.I. Hakomori, Ganglioside GM2-tetraspanin CD82 complex inhibits met and its cross-talk with integrins, providing a basis for control of cell motility through glycosynapse, J. Biol. Chem. 282 (2007) 8123–8133.
[24] S.C. Sridhar, C.K. Miranti, Tetraspanin KAI1/CD82 suppresses invasion by inhibiting integrin-dependent crosstalk with c-Met receptor and Src kinases, Oncogene 25 (2006) 2367–2378.
[25] Y. Yarden, M.X. Sliwkowski, Untangling the ErbB signalling network, Nat. Rev. Mol. Cell Biol. 2 (2001) 127–137.
[26] A.J. Ridley et al., Cell migration: integrating signals from front to back, Science 302 (2003) 1704–1709.
[27] X.A. Zhang, B. He, B. Zhou, L. Liu, Requirement of the p130CAS-Crk coupling for metastasis suppressor KAI1/CD82-mediated inhibition of cell migration, J. Biol. Chem. 278 (2003) 27319–27328.